

**Impact of climatic extremes on net subsurface discharge considering hydrologic linkage among vadose zone-unconfined aquifer-stream in Rio Grande basin**

**Project Type**

Research

**Focus Categories**

HYDROL, SW, GW

**Research Category**

Climate and Hydrologic Processes.

**Keywords**

Climate extremes, Hydrologic exchange, Net subsurface discharge, Surface-subsurface interaction.

**Start Date**

3/1/2020

**End Date**

2/28/2021

**Principal investigator(s)**

Applicant: Minki Hong (Doctoral student)

Starting / Expected year of graduation: (Fall 2017 / Summer 2021)

Address: Dept. of Biological and Agricultural Engineering, Texas A&M University,

College Station, TX 77843 Email: mkhong@tamu.edu Phone: (979) 402-4799

Advisors: Dr. Zhuping Sheng, AgriLife Research El Paso & Dr. Binayak Mohanty, BAEN

**Congressional District of the university where the work is to be conducted**

Texas District of the United States House of Representatives

**Abstract**

Increasing pressures on freshwater availability due to the rapid population growth and changing climate in the State of Texas calls for a more advanced technique to estimate and forecast its vulnerability to climatic extremes. In the present study, a newly developed predictive modeling framework is introduced to examine freshwater availability, especially in a semi-arid region in Southwest Texas. Net subsurface discharge (NSD) and streamflow, which are outputs of the modeling framework, are selected as an indicator to show freshwater vulnerability in the future. In order to represent future climatic extremes, downscaled CIMP5 RCP scenarios will be used and the impact of altered climatic variables on NSD and streamflow will be analyzed. USGS stream gauges installed along with the Rio Grande network provide stream discharge data on a sub-hourly basis, leading to the possibility of calculating measured net subsurface discharges using differential gauging method. The modeling framework calibrated for a historic baseline period 2016-2019 through the differential gauging method is providing a basis for future NSD and streamflow forecasts for the period 2020-2029. The predictions of NSD and

streamflow under different future emission scenarios can be a viable tool to examine how vulnerable the Rio Grande is against climatic extremes.

**Statement of regional or State water problem**

The population in the State of Texas has doubled since 1980, and it is expected to reach about 54 million by 2050. The rapid population growth raises concerns about freshwater availability because of its limited capacity to meet agricultural/domestic water demands across the state. On the other hand, records show that Texas is one of the water-deficient states which are highly vulnerable to drought. Several parts of Texas, especially semi-arid regions, have been experiencing hydrologic/agricultural droughts every few years (NOAA, 2019). As climatic extremes are expected to be happening more frequently under changing climate, our efforts should be made to cope with the high level of vulnerability in the regions.

From its headwaters in the San Juan Range of the Colorado Rockies to the Gulf of Mexico at Brownsville, Texas, the Rio Grande River draws from about 11 percent of the contiguous United States (CONUS), with much of that being drought-prone land (Figure 1). That vulnerability is aggravated by several dams and irrigation diversions along the river, which has left significant portions of the river dry in recent years. In 2001 the river failed to reach the Gulf of Mexico for the first time, and it happened again in 2002. As in all semi-arid to arid regions

from New Mexico-Texas, the waters of the Rio Grande River are much sought after and usually overallocated. Because of the intense agriculture from New Mexico through Texas the Rio Grande River is in demand, showing that about 75 percent of water withdrawals from the Rio Grande River are to support irrigation. The excessive use of surface waters from the Rio Grande River may also cause a high drought vulnerability.

Moreover, snowmelts from the San Juan Mountain is a significant water source for the Rio Grande river. Runoff from northern Mexico also contributes to the streamflow. These water sources, however, can be

significantly varied by year under changing climate. Because of the uncertainty that is increased by the emerging climate extremes due to climate change, our efforts to cope with the high drought-vulnerable regions in the Rio Grande basin have become more critical.

In terms of improving the capability to deal with the high drought-vulnerability in the semi-arid and arid areas in the Rio Grande basin, a better examination and understanding of water budget in watersheds is of critical importance. Also, interactions between the vadose zone, phreatic aquifer, and stream are vital components of the water budget of the river reaches.

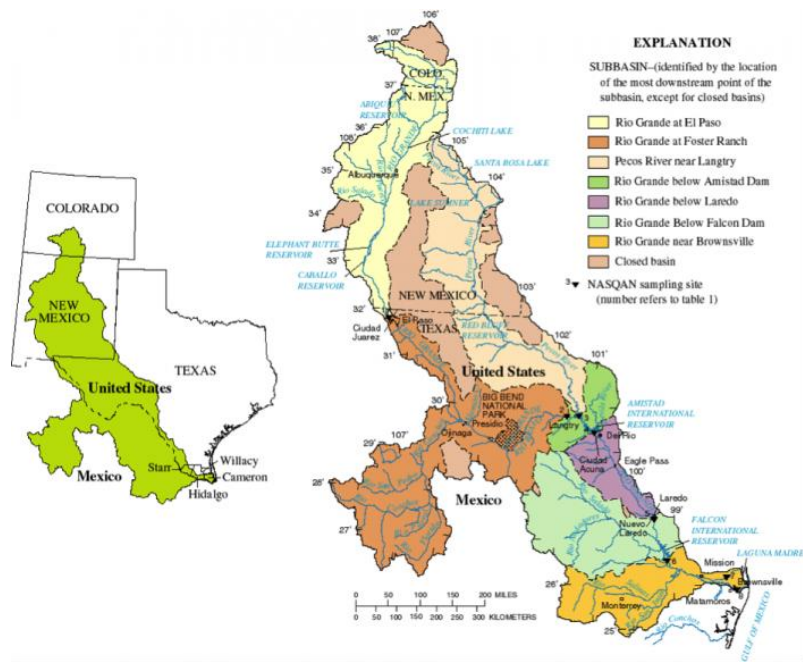


Figure 1. The drainage basin of the Rio Grande River. (Source: USGS)

Estimating NSD is of critical importance in assessing freshwater availability because it is one of the significant water budget components in stream reaches (Bouaziz *et al.*, 2018). Especially in arid or semi-arid regions, where little overland flow occurs, NSD is the critical water budget component that determines the variations of streamflow across the network of stream reaches.

**Statement of results or benefits**

Net subsurface discharge (NSD) on a daily basis will be forecasted from 2020 through 2029 (10 years) in selected Rio Grande river reaches. The forecasted information will include 1) the direction and amount of NSD in selected Rio Grande river reaches, 2) the ratio of NSD contribution to its streamflow. High-resolution mappings of soil moisture, groundwater level, and river stage will also be generated, showing how the hydrologic components are spatiotemporally distributed across catchments/sub-catchments (Figure 2).

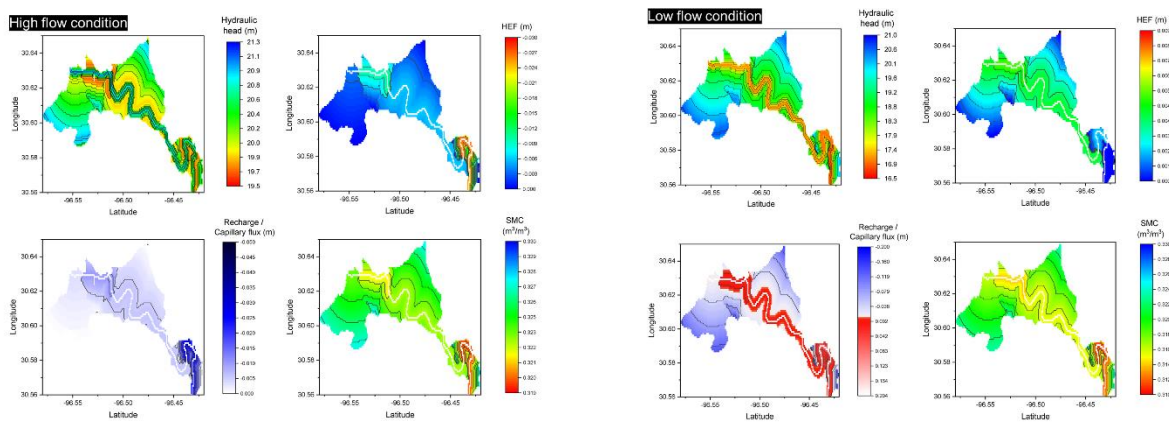


Figure 2. Examples of high-resolution mappings of hydrologic states and bidirectional fluxes such as groundwater level-river stage, soil moisture, hyporheic exchange fluxes (HEF), and groundwater recharge/capillary fluxes.

**Nature, scope, and objectives of the project, including a timeline of activities**

Estimated/forecasted NSD can be used as a viable tool to monitor the time-dependent state of 1) volume of discharge and 2) the status of stream reaches (gaining or losing). This study aims to investigate how climatic extremes will impact NSD and streamflow of river reaches in selected Rio Grande river basin under different future emission scenarios in Texas. The statistically downscaled atmospheric forcing from the twelve Coupled Model Inter-comparison Project Plan (CMIP5) will be used to generate future projected climatic variables. The climatic variables under Representative Concentration Pathway (RCP) +2.6w/m<sup>2</sup>, +4.5w/m<sup>2</sup> +6.0w/m<sup>2</sup>, and +8.5w/m<sup>2</sup> scenarios are currently available and will lead to the different soil moisture conditions, which provide boundary conditions to groundwater module. The BE3S will then simulate the variations of NSD considering time-varying hydrologic components such as soil moisture, groundwater table, streamflow as well as the impact of the variability of hydrologic state in a flow domain to other domains. The model will be operated for a historical baseline period 2015-2019 (5 years) and a future period 2020-2029 (10 years). Differential gauging method, a proven method to directly measure NSD, will also be performed to assess the accuracy of NSD simulations. The differential gauging method needs streamflow (discharge) data measured at upstream and downstream in a single reach, and thus streamflow data that has been measured by USGS stream gauges for the historic baseline period will be utilized. Then the model will be calibrated and validated through the comparison between observational and

simulated NSD, and then predictions of NSD and stream in the future period will be generated. The predictions of NSD and streamflow under different future emission scenarios can be used as an indicator showing how vulnerable (or resilient) the Rio Grande river is under the expected climatic extremes.

Task	Inputs	Output	Timeline
1.Data acquisition		-NHDPlus v2.0 -Atmospheric forcing (CMIP5) -USGS observations	Jan – Feb 2020
2.Model set up 3.Model calibration	-Modeling framework -CMIP5 forcing data for 2016-2019 - USGS observations	-Model calibration -NSD and streamflow simulations for baseline period	Mar – Jun 2020
4.Model validation	-Modeling framework -CMIP5 forcing data for 2020-2029 - USGS observations	-Model validation -NSD and streamflow predictions for future period	Jul – Sep 2020
5.Result analysis 6.Final report	-Predictions of NSD and streamflow - USGS observations	-Statistical analysis of model’s performance -Examination of vulnerability of Rio Grande	Oct – Dec 2020

**Methods, procedures, and facilities**

This study will be a continuation of the on-going USDA-NIFA project, which focuses on assessing the hydrology and freshwater availability of the Rio Grande basin’s water resources. As an effort to better represent the interactive flow processes within surface and subsurface waters, a forward predictive modeling scheme was developed and verified over several stream reaches in Brazos River basin, TX (Figure 3). The model represents the simultaneous interactions among vadose zone-phreatic aquifer-stream by fully connecting three different governing equations through boundary condition-based coupling approach. This newly developed modeling scheme, named BE3S (Bidirectional Exchange Scheme in Surface and Subsurface), can track the direction and amount of two-way exchange fluxes such as groundwater recharge, capillary flux, and hyporheic exchange flux (HEF). Net subsurface discharge (NSD), which is the cumulative HEFs over travel time at a reach, was successfully predicted and verified against measured NSD (Hong et al., 2019). These available results demonstrate the model’s capability to predict NSD and other exchange fluxes in semi-arid regions.

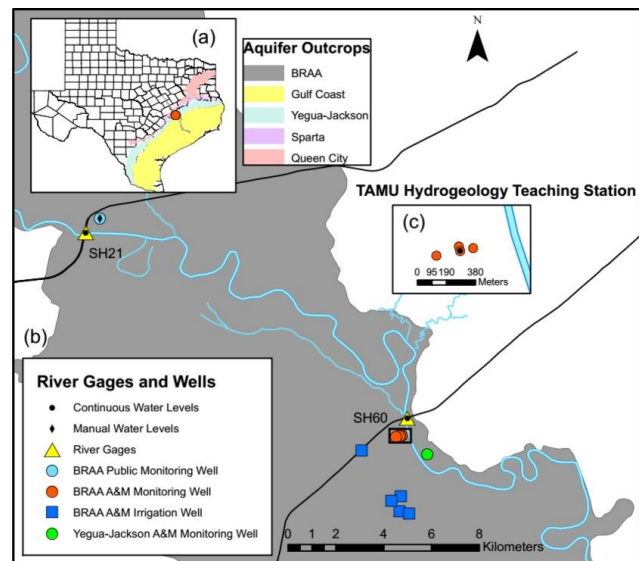


Figure 3. A study area used to test the BE3S modeling framework to verify its predictive performance.

The dynamics of each flow domain can be represented by individual PDE corresponding to that flow domain. The use of different PDEs to represent each flow process can lead to the explicit and individual representation of the dynamics of the boundary conditions (interfacial and external), and can also provide the basis for simulating bidirectional exchange fluxes between vadose zone-unconfined aquifer, and unconfined aquifer-river through the fully connected boundaries between multiple flow domains (Figure 4).

## 1. Governing equations

Richards' equation, Boussinesq equation, and Saint-Venant equation are selected to explicitly represent soil water infiltration/redistribution, groundwater level dynamics, and open channel flow, respectively.

### 1.1 Richards' equation

One-dimensional head-based

Richards equation (RE) is used to describe the dynamics of soil moisture in a vertical direction. RE has been widely used to simulate soil moisture movement in the vadose zone (Hornberger & Remson, 1970; Kumar, Duffy, & Salvage, 2009; Van Dam & Feddes, 2000). RE in the vertical direction can be written as Equation (1).

$$C(h) \frac{\partial h}{\partial t} = \frac{\partial}{\partial z} \left[ k(h) \left( \frac{\partial h}{\partial z} + 1 \right) \right] \quad (1)$$

where  $t$  is time ( $T$ ),  $z$  is the vertical coordinate (positive downward) ( $L$ ),  $h$  denotes soil water pressure head ( $L$ ),  $C(h)$  denotes the differential water capacity ( $\frac{d\theta}{dh}$ ) ( $L^{-1}$ ),  $K(h)$  is unsaturated hydraulic conductivity ( $LT^{-1}$ ). Since RE is one-dimensional, no lateral communication between soil columns is considered. The degree of saturation  $S_e(\psi)$  and relative permeability  $K_r(S_e)$ , required for modeling  $C(h)$  and  $K(h)$ , is described by Mualem-van Genuchten formulation (Equation 2, 3).

$$S_e(\psi) = \frac{\theta - \theta_r}{\theta_s - \theta_r} = (1 + (\alpha\psi)^n)^{-m} \quad (2)$$

$$K_r(S_e) = S_e^l \left[ \frac{\int_0^{S_e} \frac{1}{\psi(S_e)} dS_e}{\int_0^1 \frac{1}{\psi(S_e)} dS_e} \right]^2 \quad (3)$$

Where  $\theta$  is the volumetric water content ( $L^3L^{-3}$ ),  $\theta_s$  and  $\theta_r$  are saturated and residual volumetric water content, respectively ( $L^3L^{-3}$ ).  $\psi$  is the water potential ( $L$ ).  $\alpha$  is the parameter related to the inverse of the air-entry pressure ( $L^{-1}$ ), and  $l$  is the tortuosity parameter assumed to be 0.5.  $n$  is a measure of the pore size distribution and  $m$  is  $1 - 1/n$ .

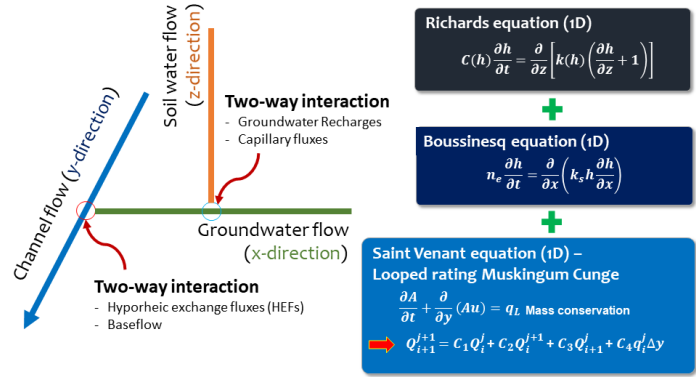


Figure 4. Schematic of coupled governing equations system. Richards' equation on the  $x$  coordinate, Boussinesq equation on the  $y$  coordinate, and Saint-Venant equation on the  $z$  coordinate.

## 1.2 Boussinesq equation

One-dimensional Boussinesq equation (BE) is a proven PDE to model unconfined groundwater flow in a horizontal aquifer (Basha, 2013; Hornberger, Ebert, & Remson, 1970; Tolikas, Sidiropoulos, & Tzimopoulos, 1984). BE can represent the interactive flow process between the river and local unconfined aquifer if the river stage is applied to one-dimensional BE as a time-dependent boundary condition (Di et al., 2011). In the present work, non-linear BE is used instead of linearized one to get more accurate traveling wave solution of groundwater table position in the subsurface, and the non-linear BE is applied in a direction perpendicular to the flow direction of river to use time-varying river stage as one of the boundary conditions of BE (Equation 4).

$$n_e \frac{\partial H}{\partial t} = K_s \frac{\partial}{\partial x} \left( H \frac{\partial H}{\partial x} \right) \quad (4)$$

Where  $x$  is the horizontal coordinate ( $L$ ),  $H$  is hydraulic head at which GWT is positioned ( $L$ ),  $n_e$  is effective or drainable porosity (-),  $K_s$  is saturated hydraulic conductivity ( $LT^{-1}$ ).

## 1.3 Saint-Venant equation

For river channel flow, the Saint-Venant equation (SVE) is used (Equation 5). Non-homogeneous SVE equation is solved by the Looped rating Muskingum-Cunge method, and thus only mass is conserved. The Looped rating Muskingum-Cunge method solves the continuity equation of SVE rating the looped curve, which is mainly caused by the slope of a river reach. This extended Muskingum-Cunge model can better represent diffusion routing of flood wave by incorporating water surface slope and Vedernikov number into Reynolds number calculation (Ponce & Lugo, 2001). SVE derived from the Looped rating Muskingum-Cunge method can be written as Equation (6).

$$\frac{\partial A}{\partial t} + \frac{\partial Au}{\partial y} = q \quad (5)$$

$$Q_{i+1}^{j+1} = C_1 Q_i^j + C_2 Q_i^{j+1} + C_3 Q_{i+1}^j + C_4 q_i^j \Delta y \quad (6)$$

Where  $A$  is the cross-sectional area of the flow at location  $y$  ( $L^2$ ),  $u$  is flow velocity ( $LT^{-1}$ ),  $Q_i^j$  denotes the estimated stream discharge at  $j$ th time step on  $i$ th stream node ( $L^3T^{-1}$ ),  $\Delta y$  is the distance between adjacent stream nodes ( $L$ ).  $q_i^j$  is groundwater-surface exchange resulting from the hydraulic gradient between a river reach and local aquifer at  $j$ th time step on  $i$ th stream node ( $L^2T^{-1}$ ).  $C_1, C_2, C_3, C_4$  are time-dependent routing coefficient determined by channel geometry and flow conditions (-). As the equation is a one-dimensional explicit scheme, however, backwater and localized effects are not accounted for in the modeling framework. Also, the Manning formula is used to calculate channel wave celerity and infer stream discharge (Equation 7).

$$Q = VA = \frac{1}{m} AR_n^{2/3} S^{1/2} \quad (7)$$

Where  $m$  the roughness coefficient in Manning formula and  $S$  is the slope of the channel ( $L^{-1}$ ). Mean velocity derived from the Manning equation is used to infer travel time, stream discharge, and river stage along the stream reach. As a result, streamflow hydrographs at the inlet and outlet of each catchment can be established.



## 2 Boundary-condition based coupling approach

A complete coupled surface-subsurface flow system should include surface and subsurface hydrologic components, interfacial and external boundary conditions, and initial conditions within the modeling framework (Furman, 2008). To model the bidirectional exchange between the vadose zone-unconfined aquifer-river explicitly, it is essential to fully connect the vadose zone-unconfined aquifer-river while accounting for the dynamic condition of the flow domains. In the present work, the hydrologic states and fluxes in (and between) the flow domains will be used to establish an interfacial boundary equation to connect the dynamic flow domains. Two-way exchange fluxes between vadose zone-unconfined aquifer (i.e., groundwater recharge and capillary flux) will be used to set up the interfacial boundary equation representing time-varying hydrologic states of the two flow domains (Equation 8).

$$D_i^{j+1} = H_i^j - \nabla f_{vp}^{j+1} \times A_v \quad (8)$$

Where  $D_i^j$  is the interaction depth between vadose zone and unconfined aquifer (IDVU) at  $j$  th time step on  $i$  th aquifer node from the river ( $L$ ).  $H_i^j$  is the hydraulic head of GWL at  $j$ th time step on  $i$  th node from a river reach.  $\nabla f_{vp}^j$  denotes net exchange fluxes between vadose zone-unconfined aquifer (downward positive,  $LT^{-1}$ ) at  $j$  th time step and  $A_v$  is the area of a grid cell in soil column. As indicated in Figure 4, groundwater level (GWL) is decided in two steps.

1) The interaction depth between vadose zone-unconfined aquifer (IDVU) is calculated by subtracting net exchange between vadose zone-unconfined aquifer ( $\nabla f_{vp}$ ) from the hydraulic head of GWL at the previous time step (Equation 8), yielding horizontal  $D_i$  profile from a river reach. 2) The horizontal profile of  $D_i$  is used as an initial condition for BE solutions ( $H_i$ ) while using the time-dependent river stage as a boundary condition (Figure 5). This horizontal  $H_i$  profile is regarded as hydraulic heads of GWL on each groundwater grid cell at the corresponding time step. As mentioned, the time-dependent river stage is incorporated into BE as a boundary condition to simulate the response of the groundwater level to the time-varying river stage (Equation 9).

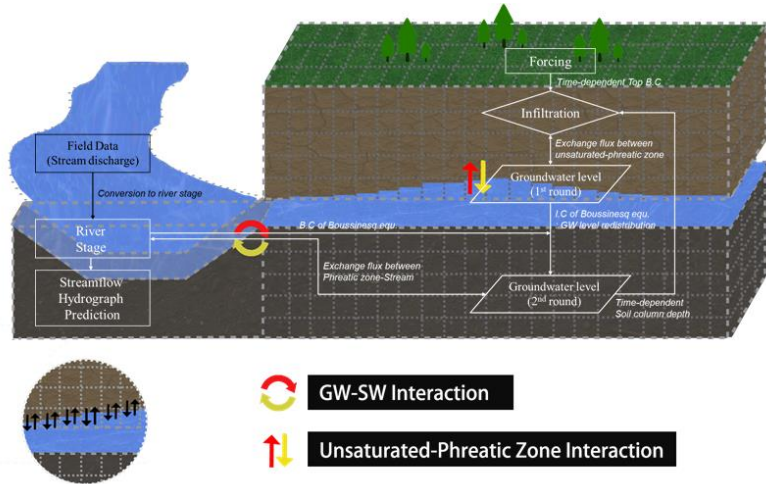


Figure 5. Modeling framework that shows how the hydrologic states of soil moisture, groundwater, and streamflow are decided with respect to bidirectional exchange fluxes between vadose zone-unconfined aquifer-river.

$$n_e \frac{H_i^{j+1} - H_i^j}{\Delta t} = \frac{K_s}{\Delta x} \left[ H_i^j \left( \frac{H_{i+1}^j - H_i^j}{\Delta x} \right) - H_{i-1}^j \left( \frac{H_i^j - H_r^j}{\Delta x} \right) \right] \quad (i = 1) \quad (9)$$

$$n_e \frac{H_i^{j+1} - H_i^j}{\Delta t} = \frac{K_s}{\Delta x} \left[ H_i^j \left( \frac{H_{i+1}^j - H_i^j}{\Delta x} \right) - H_{i-1}^j \left( \frac{H_i^j - H_{i-1}^j}{\Delta x} \right) \right] \quad (i = 2, \dots, n) \quad (10)$$

Where  $H_i^j$  is the hydraulic head of GWL at  $j$  th time step on  $i$  th node ( $L$ ).  $H_r^j$  is the river stage at  $j$  th time step ( $L$ ),  $\Delta x$  is the size of a grid cell in the unconfined aquifer ( $L$ ). Vadose zone and unconfined aquifer are spatially discretized with structured finite volume and finite difference technique while sharing the same area of a grid cell so that  $\Delta x^2$  is equal to  $A_p$ . The initial condition ( $D^j$ ) is decided at each time step by Equation (8) using  $H_i^j$  from Equation (9), (10), yielding the eventual position of groundwater level at  $j+1$  th time step ( $H_i^{j+1}$ ). The boundary condition at which the unconfined aquifer is connected with a stream is set to a time-dependent boundary condition (Dirichlet type) using river stage data, and the boundary condition on the other side is configured as zero-flux boundary condition. As can be seen from Figure 6, the spatial domain of soil column is decided in accordance with the position of groundwater level at the corresponding time step. Since the soil column is discretized with the same number of grid cells ( $n$ ) the height of a soil grid cell ( $\Delta z$ ) is also a time-dependent variable ( $\Delta z^j = D^j/n$ ). Structured cell-centered finite volume grids and implicit backward Euler methods are used for spatial and temporal discretization of the soil column, respectively (Equation 11).

$$C(h)_{i+\frac{1}{2}}^{j+1} \frac{h_i^{j+1} - h_i^j}{\Delta t} \quad (i = 1, 2, \dots, n) \quad (11)$$

$$= \left[ \frac{K(h)_{i+\frac{1}{2}}^{j+1} \left( \frac{h_{i+1}^{j+1} - h_i^{j+1}}{z_{i+1} - z_i} \right) - K(h)_{i-\frac{1}{2}}^{j+1} \left( \frac{h_i^{j+1} - h_{i-1}^{j+1}}{z_i - z_{i-1}} \right)}{\Delta z^j} \right] + \left[ \frac{K(h)_{i+\frac{1}{2}}^{j+1} - K(h)_{i-\frac{1}{2}}^{j+1}}{\Delta z^j} \right]$$

Since  $K(h)$  spans several orders of magnitude, the determination of interfacial unsaturated hydraulic conductivity  $K(h)_{i+1/2}$  is of importance for numerical stability. In this study  $K(h)_{i+1/2}$  is calculated once the hydraulic conductivity at each center node of soil grid cells is calculated, and then logarithmic mean between adjacent soil grid cells is calculated as interfacial unsaturated hydraulic conductivity. Because of the nature of applying boundary condition with finite volume discretization, the top and bottom nodes can be accurately located at the land surface and groundwater level respectively, ensuring that the hydraulic head at the bottom boundary condition of the vadose zone is perfectly matched to the hydraulic head at which groundwater level is positioned (Figure 6). The bottom boundary condition of Equation (11) is set to near-zero matric potential to assume that the bottom of soil columns is connected to the unconfined aquifer. The top boundary condition is given by matric potential changing over time according to surface soil moisture. Also, the river routing module is configured to rely on

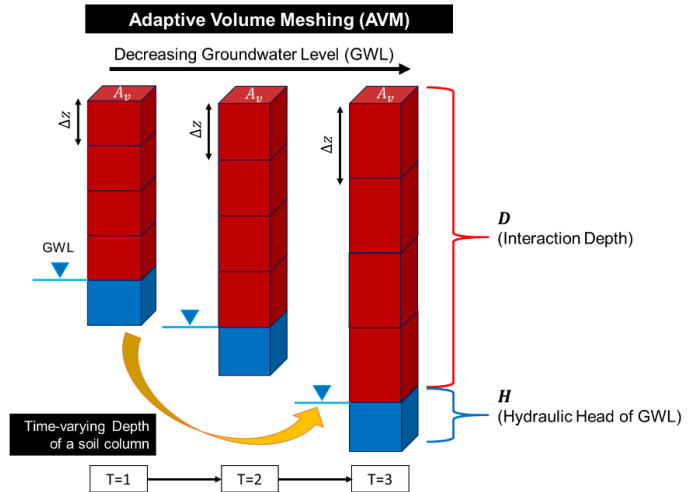


Figure 6. An example schematic of defining subsurface variables  $D$ ,  $H$ , and height of a soil grid cell according to time-varying GWL condition using the Adaptive Volume Meshing (AVM) technique



the NHDPlus v2.0 river network, whose exchange with groundwater ( $q$ ) is calculated using the conductance concept (Equation 12). National Hydrography Dataset (NHDPlus v2.0) is an integrated suite of application-ready geospatial data products. It produces geospatial data such as National Elevation Dataset (NED), watershed boundary dataset, and flowline of river reaches. In the present work, the NHDPlus v2.0 dataset is used to delineate river reaches and define catchment boundaries across CONUS, leading to the possibility to analyze the entire U.S. into catchments (USGS, 2012).

$$\nabla f_{pr}^j = \begin{cases} K_r \left[ (W_r^j + 2H_r^j) \times \left( \frac{H_r^j - H_{M_r}^j}{M_r} \right) \right] \times \Delta t & (H_x^j > -M_r) \\ K_r \left[ (W_r^j + 2H_r^j) \times \left( \frac{H_r^j - M_r}{M_r} \right) \right] \times \Delta t & (H_x^j \leq -M_r) \end{cases} \quad (12)$$

Where  $K_r$  is hydraulic conductivity of river bottom sediment ( $LT^{-1}$ ),  $M_r$  is the thickness of river bottom sediment ( $L$ ),  $W_r^j$  is wetted perimeter to at  $j$  th time step ( $L$ ),  $H_{M_r}^j$  is the hydraulic head of GWL at a distance of  $M_r$  from a river channel at  $j$  th time step ( $L$ ).

### 3 Temporal coupling

Integrated hydrologic models that handle multiple processes typically involve different temporal scales that could range from an hour to years. Especially when dealing with a coupled PDEs system determination of temporal scales for each flow process must be sensitive to maintain the numerical stability of the entire system. Surface water requires a faster temporal scale than subsurface flow due to the differences in wave propagation. The connected system of groundwater flow is therefore solved on a daily basis, and the soil water flow and channel flow are solved on an hourly basis. Successful matching up of different temporal scales while respecting mass balance and numerical stability heavily depends on how a variety of hydrologic states and fluxes at  $j$  th time step are used to define boundary conditions at  $j+1$  th time step. The steps are given as follows.

- 1) Soil water flow is solved on an hourly basis with the top (time-dependent matric potential) and bottom boundary condition (near-zero matric potential).
- 2) The cumulative exchange fluxes between vadose zone-unconfined aquifer ( $\nabla f_{vp}^j$ ) during 24-hours (1-day) is used to define the initial condition ( $D_i^j$ ) for BE solutions ( $H_i^j$  ( $i = 1, 2, \dots, k$ )).  $k$  is the number of aquifer grids.
- 3) After  $H_i^j$  ( $i = 1, 2, \dots, k$ ) is yielded, the exchange between the river and the unconfined aquifer is calculated (Equation 12) using  $H_{M_r}^j$  and daily estimates of the river stage at  $j$  th time step.
- 4) The exchange between river and aquifer ( $\nabla f_{pr}^j$ ) is assumed to occur at a constant rate during a day so that  $\nabla f_{pr}^j$  is divided by 24 (hours) yielding  $q^j$ .
- 5) River stage profile along the corresponding reach is calculated on an hourly-basis using  $q^j$ , and the estimate at the last time step (24<sup>th</sup>) is considered as the modeled output of the river stage profile.

To yield model outputs on a daily-basis river-unconfined aquifer exchange variable ( $q$ ), which is calculated using daily estimates of river and groundwater level, is assumed to occur at a constant rate during a day so that  $\nabla f_{pr}^j$  is divided by 24 (hours). The net exchange flux between the vadose zone and unconfined aquifer ( $\nabla f_{vp}^j$ ) is the cumulative exchange fluxes that occur during a day, also the net exchange flux between unconfined aquifer and river ( $\nabla f_{pr}^j$ ) yielded with daily river stage and groundwater level data is divided by 24 to get lateral exchange fluxes ( $q_L$ ) on an hourly basis to be used in looped-rating Muskingum-Cunge (Equation 6).

#### 4 Domain configuration and setup

The boundaries of aquifer and catchment follow the NHDPlus v2.0 catchment boundaries. Thus the number of aquifer grid cells for BE depends on the size of each catchment. Each aquifer grid cell is assigned the minimum Euclidean distance from a river reach. The distributions of  $D$  values (Equation 8) are estimated according to the distance from the channel. For example  $D_1$  denotes  $D$  values at which 1 grid away from a channel. Relying on each distribution of  $D_i$  ( $i = 1, \dots, k$ ) expectation of  $D_i$  ( $E[D_i]$ ) is calculated to decide the interfacial boundary equation at that time step. Then the BE solutions  $H_i^j$  ( $i = 1, \dots, k$ ) are remapped following the aquifer grid's distance from a channel (Figure 7).

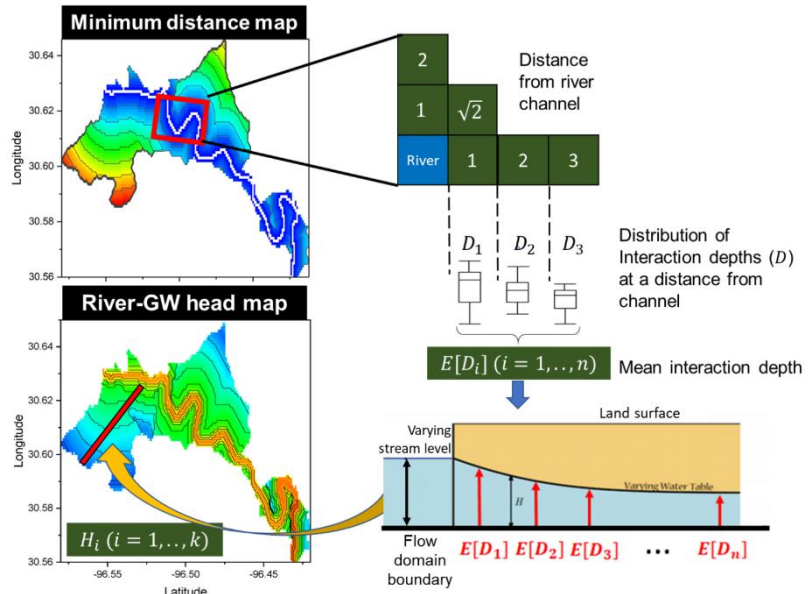


Figure 7. Modeling domain configuration and setup to represent horizontal groundwater wave propagation within a catchment boundary.

Then the BE solutions  $H_i^j$  ( $i = 1, \dots, k$ ) are remapped following the aquifer grid's distance from a channel (Figure 7).

#### Related research

In most process-based integrated hydrologic models, however, a numerical scheme used to represent the surface-subsurface interaction relies on loose-coupling so that only one-way exchange flux between flow domains can be simulated, which is not realistic. In terms of stream-aquifer interaction, for example, only groundwater discharge (exchange from an aquifer to stream) can be taken into account due to the loose-coupling, implying that streams are always considered as gaining stream irrespective of hydrologic states of the two flow domains. Even though several integrated models tried to calculate two-way exchange fluxes through the conductance concept, inter-facial boundary equations that define the spatial domain of each flow regime are found not to be updated over time in the models. This disregard of the time-dependent position of inter-facial boundaries between surface and subsurface could result in the inaccuracy of exchange flux estimations. Moreover, for the studies that attempted to describe the interaction

of stream-aquifer in a land surface model, all of them showed that a two-way exchange between the phreatic aquifer and vadose zone is not represented, and none of the time-varying condition of interfaces between the two domain is considered.

A variety of schemes that represent the exchange fluxes between different water storages have been developed and also integrated with the LSMs. To incorporate groundwater dynamics into a land surface flow processes, the groundwater system has been often described as a non-linear reservoir that can model time-dependent groundwater storage according to recharge from the overlying soils and discharges into streams (Koirala, Yeh, Hirabayashi, Kanae, & Oki, 2014; NCAR, 2018; Yeh & Eltahir, 2005). Because of the lack of physics that links surface water dynamics to groundwater storage, however, only one-way communication from ground storage to rivers is considered based on a non-linear function. If the groundwater system is assumed to be steady-state for evaluating only the long-term effect, the temporal variability of GWL in a fine-scale (e.g., daily) cannot be considered (Fan, Miguez-Macho, Weaver, Walko, & Robock, 2007). There was a study that tried to represent groundwater-surface interaction by incorporating the Dupuit approximation (Zeng et al., 2016), however, the effect of groundwater recharge on the GWL variations is not considered so that the comprehensive understanding of moisture fluxes exchange among vadose zone-unconfined aquifer-river was not feasible (Kong et al., 2015). Several other studies tried to integrate dynamic groundwater model with land surface flow processes relying on process-based concept (Bisht et al., 2017; Maxwell & Miller, 2005; G.-Y. Niu et al., 2014; J. Niu, Shen, Chambers, Melack, & Riley, 2017). Since such models often rely on process-based framework, however, they have several limitations:

- 1) the time-varying boundary conditions is not explicitly represented so that the impact of changing the spatial extent of each flow domain on model states and fluxes cannot be evaluated.
- 2) High computational demands are often required to solve complex GWL dynamics in the coupled groundwater model.
- 3) Significant discrepancies exist in their results when the models are applied to highly non-linear problems due to the differences in their modeling of exchange fluxes

Therefore, it is needed to develop an improved forward scheme that 1) represents GWL dynamics resulting from bidirectional interactions between vadose zone-unconfined aquifer-rivers, 2) explicitly simulate time-dependent boundary conditions (external, interfacial) that affect both model states and fluxes, 3) computationally efficient eliminating the need to solve complex groundwater flow equation.

### ***Training potential***

PI will conduct all the tasks across the entire duration (3/1/2020 – 2/28/2021), collaborating with a graduate student (doctoral student) to accomplish the goal of the project.

# MINKI HONG

233C Scoates Hall 2117 TAMU · (+1) 979.402.4799

[mkhong@tamu.edu](mailto:mkhong@tamu.edu)

## EDUCATION

**2017 – PRESENT**

**DOCTORAL STUDENT**, TEXAS A&M UNIVERSITY

Graduate Research Assistant

Biological and Agricultural Engineering Department

**2014 – 2016**

**MASTER OF SCIENCE**, SEOUL NATIONAL UNIVERSITY

Department of Landscape Architecture and Rural System Engineering

(Rural System Engineering Major)

**2008 – 2014**

**BACHELOR OF SCIENCE**, SEOUL NATIONAL UNIVERSITY

Department of Landscape Architecture and Rural System Engineering

(Rural System Engineering Major)

## RESEARCH INTERESTS

- Numerical module development and modeling
- Coupled processes between surface-subsurface
- Earth system modeling
- Data assimilation

## PROJECTS

**2017 – PRESENT**

**SUSTAINABLE WATER RESOURCES FOR IRRIGATED AGRICULTURE IN A DESERT BASIN  
FACING CLIMATE CHANGE AND COMPETING DEMANDS**

United States Department of Agriculture (USDA) – National Institute of Food and Agriculture (NIFA)

**2017 – PRESENT**

**TEXAS WATER OBSERVATORY (TWO)**

Texas A&M University & Texas A&M Agrilife Research

**2014 – 2016**

**DEVELOPMENT OF WATER USE INFORMATION FORECASTING SYSTEM FOR  
AGRICULTURAL ECO-SYSTEM MANAGEMENT**

Seoul National University & National Center for Agro-Meteorology (NCAM)

**2013 – 2014**

## DEVELOPMENT OF INTELLIGENT SYSTEM FOR MANAGEMENT OF IRRIGATION AND DRAINAGE

Seoul National University & Korea Institute of Planning and Evaluation for Technology in Food, Agriculture and Fisheries (IPET)

### PUBLICATIONS

- [4] Hong, M., B. Mohanty, Z. Sheng, 2020. **An explicit scheme to represent the bidirectional exchanges among vadose zone, phreatic aquifer, and river**, *Advances in Water Resources*, [In preparation].
- [3] Hong, M., S. H. Lee, S. J. Lee, J. Y. Choi, 2019. **Application of high-resolution meteorological data from NCAM-WRF to analyze soil moisture deficit and drought severity in small-scale farmlands**, *Agricultural Water Management*, [In review].
- [2] Hong, M., R. Karki, J. M. Krienert, S. S. Memari, 2018. **Evaluating Alternative Groundwater Discharge Estimations for Improved National Water Model Forecasting**, *National Water Center Innovators Program Summer Institute Report 2018 (CUAHSI & NOAA)*.
- [1] Hong, M., S. H. Lee, J. Y. Choi, S. H. Lee, S. J. Lee, 2015. **Estimation of Soil Moisture and Irrigation Requirement of Upland using Soil Moisture Model applied WRF meteorological data**, *The Korean Society of Agricultural Engineering*.

### HONORS AND AWARDS

- [8] **USGS TWRI Grad Student Scholarship** (2020 – 21).  
*United States Geological Survey (USGS) & Texas Water Resources Institute (TWRI)*
- [7] **Soil Science Society of America Oral Presentation Award** (2019).  
*Soil Science Society of America (SSSA)*
- [6] **BAEN Graduate Student Competitive Scholarship** (2019)  
*Texas A&M University*
- [5] **Aggies Commit Fellowship** (2019)  
*Texas A&M University*
- [4] **National Water Center Summer Institute Program** (2018)  
*National Oceanic and Atmospheric Administration (NOAA)*
- [3] **BAEN Graduate Student Competitive Scholarship** (2018)  
*Texas A&M University*
- [2] **Outstanding Paper Presentation Award** (2015)  
*Korean Water Resources Association*
- [1] **Best Oral Presentation Award** (2014)  
*International Society of Paddy and Water Environment Engineering (PAWEES)*

### RELEVANT SKILLS

- Programming (Python, C, R, Mathematica)
- Linux-based high-performance computing
- Integrated modeling. Skillful at *WRF-hydro, Noah-MP, VIC (open source) Hydrus, MODFLOW (commercial) models*
- *Data visualization*



## BUDGET BREAKDOWN

Cost Category	Federal	Non-Federal	Total
1. Salaries and Wages	\$		\$
- <u>Principal Investigator(s)</u>			
- <u>Graduate Student(s)</u>		\$ 5,376	
- <u>Undergraduate Student(s)</u>			
- <u>Others</u>			
Total Salaries and Wages			
2. Fringe Benefits			
- <u>Principal Investigator(s)</u>			
- <u>Graduate Student(s)</u>		\$ 978	
- <u>Undergraduate Student(s)</u>			
- <u>Others</u>			
Total Fringe Benefits			
3. Tuition			
- <u>Graduate Student(s)</u>			
- <u>Undergraduate Student(s)</u>	\$5,000		
Total Tuition			
4. Supplies			
5. Equipment			
6. Services or Consultants			
7. Travel			
8. Other direct costs			
9. Total direct costs		\$ 6,668	
10a. Indirect costs on federal share	XXXXXXXX XXXXXXXX		
10b. Indirect costs on non-federal share	XXXXXXXX XXXXXXXX	\$ 3,334	
11. Total estimated costs	\$ 5,000	\$ 10,002	\$
Total Costs at Campus of the University on which the Institute or Center is located.	\$ 5,000	\$ 10,002	\$
Total Costs at other University Campus Name of University:	\$	\$	\$

## BUDGET JUSTIFICATION

<p><b>Salaries and Wages for PIs.</b> Provide personnel, title/position, estimated hours and the rate of compensation proposed for each individual.</p>
<p><b>Salaries and Wages for Graduate Students.</b> Provide personnel, title/position, estimated hours and the rate of compensation proposed for each individual. (Other forms of compensation paid as or in lieu of wages to students performing necessary work are allowable provided that the other payments are reasonable compensation for the work performed and are conditioned explicitly upon the performance of necessary work. Also, note that tuition has its own category below and that health insurance, if provided, is to be included under fringe benefits.)</p>
<p><b>Salaries and Wages for Undergraduate Students.</b> Provide personnel, title/position, estimated hours and the rate of compensation proposed for each individual. (Other forms of compensation paid as or in lieu of wages to students performing necessary work are allowable provided that the other payments are reasonable compensation for the work performed and are conditioned explicitly upon the performance of necessary work. Also, note that tuition has its own category below and that health insurance, if provided, is to be included under fringe benefits.)</p>
<p><b>Salaries and Wages for Others.</b> Provide personnel, title/position, estimated hours and the rate of compensation proposed for each individual.</p>
<p><b>Fringe Benefits for PIs.</b> Provide the overall fringe benefit rate applicable to each category of employee proposed in the project. . Note: include health insurance here, if applicable.</p>
<p><b>Fringe Benefits for Graduate Students.</b> Provide the overall fringe benefit rate applicable to each category of employee proposed in the project. Note: include health insurance here, if applicable.</p>
<p><b>Fringe Benefits for Undergraduate Students.</b> Provide the overall fringe benefit rate applicable to each category of employee proposed in the project. Note: include health insurance here, if applicable</p>
<p><b>Fringe Benefits for Others.</b> Provide the overall fringe benefit rate applicable to each category of employee proposed in the project. . Note: include health insurance here, if applicable.</p>
<p><b>Tuition for Graduate Students.</b> The total amount of \$5,000 will be used to support PI's tuition for the 2020 spring/fall semester.</p>
<p><b>Tuition for Undergraduate Students</b></p>
<p><b>Supplies.</b> Indicate separately the amounts proposed for office, laboratory, computing, and field supplies. Provide a breakdown of the supplies in each category.</p>
<p><b>Equipment.</b> Identify non-expendable personal property having a useful life of more than one (1) year and an acquisition cost of more than \$5,000 per unit. If fabrication of equipment is proposed, list parts and materials required for each, and show costs separately from the other items. A detailed breakdown is required.</p>
<p><b>Services or Consultants.</b> Identify the specific tasks for which these services, consultants, or subcontracts would be used. Provide a detailed breakdown of the services or consultants to include personnel, time, salary, supplies, travel, etc.</p>
<p><b>Travel.</b> Provide purpose and estimated costs for all travel. A breakdown should be provided to include location, number of personnel, number of days, per diem rate, lodging rate, mileage and mileage rate, airfare (whatever is applicable).</p>
<p><b>Other Direct Costs.</b> Itemize costs not included elsewhere, including publication costs. Costs for services and consultants should be included and justified under "Services or Consultants (above). Please provide a breakdown for costs listed under this category.</p>
<p><b>Indirect Costs.</b> Provide negotiated indirect ("Facilities and Administration") cost rate.</p>

## Attachment C – Focus Categories

ACID DEPOSITION	ACD
AGRICULTURE	AG
CLIMATOLOGICAL PROCESSES	CP
CONSERVATION	COV
DROUGHT	DROU
ECOLOGY	ECL
ECONOMICS	ECON
EDUCATION	EDU
FLOODS	FL
GEOMORPOLOGICAL PROCESSES	GEOMOR
GEOCHEMICAL PROCESSES	GEOCHE
GROUNDWATER	GW
HYDROGEOCHEMISTRY	HYDGEO
HYDROLOGY	HYDROL SW GW
INVASIVE SPECIES	INV
IRRIGATION	IG
LAW, INSTITUTIONS, AND POLICY	LIP
MANAGEMENT AND PLANNING	M&P
METHODS	MET
MODELS	MOD
NITRATE CONTAMINATION	NC
NON POINT POLLUTION	NPP
NUTRIENTS	NU
RADIOACTIVE SUBSTANCES	RAD
RECREATION	REC
SEDIMENTS	SED
SOLUTE TRANSPORT	ST
SURFACE WATER	SW
TOXIC SUBSTANCES	TS
TREATMENT	TRT
WASTEWATER	WW
WATER QUALITY	WQL
WATER QUANTITY	WQN
WATER SUPPLY	WS
WATER USE	WU
WETLANDS	WL

## References

- Basha, H. A. (2013). Traveling wave solution of the Boussinesq equation for groundwater flow in horizontal aquifers. *Water Resources Research*, 49(3), 1668-1679. doi:10.1002/wrcr.20168
- Bisht, G., Huang, M. Y., Zhou, T., Chen, X. Y., Dai, H., Hammond, G. E., . . . Zachara, J. M. (2017). Coupling a three-dimensional subsurface flow and transport model with a land surface model to simulate stream-aquifer-land interactions (CP v1.0). *Geoscientific Model Development*, 10(12), 4539-4562. doi:10.5194/gmd-10-4539-2017
- Di, Z. H., Xie, Z. H., Yuan, X., Tian, X. J., Luo, Z. D., & Chen, Y. N. (2011). Prediction of water table depths under soil water-groundwater interaction and stream water conveyance. *Science China-Earth Sciences*, 54(3), 420-430. doi:10.1007/s11430-010-4050-8
- Fan, Y., Miguez-Macho, G., Weaver, C. P., Walko, R., & Robock, A. (2007). Incorporating water table dynamics in climate modeling: 1. Water table observations and equilibrium water table simulations. *Journal of Geophysical Research-Atmospheres*, 112(D10). doi:10.1029/2006jd008111
- Furman, A. (2008). Modeling Coupled Surface-Subsurface Flow Processes: A Review. *Vadose Zone Journal*, 7(2), 741. doi:10.2136/vzj2007.0065
- Hornberger, G. M., Ebert, J., & Remson, I. (1970). NUMERICAL SOLUTION OF BOUSSINESQ EQUATION FOR AQUIFER-STREAM INTERACTION. *Water Resources Research*, 6(2), 601-+. doi:10.1029/WR006i002p00601
- Hornberger, G. M., & Remson, I. (1970). A MOVING BOUNDARY MODEL OF A ONE-DIMENSIONAL SATURATED-UNSATURATED, TRANSIENT POROUS FLOW SYSTEM. *Water Resources Research*, 6(3), 898-+. doi:10.1029/WR006i003p00898
- Koirala, S., Yeh, P. J. F., Hirabayashi, Y., Kanae, S., & Oki, T. (2014). Global-scale land surface hydrologic modeling with the representation of water table dynamics. *Journal of Geophysical Research-Atmospheres*, 119(1), 75-89. doi:10.1002/2013jd020398
- Kong, J., Xin, P., Hua, G. F., Luo, Z. Y., Shen, C. J., Chen, D., & Li, L. (2015). Effects of vadose zone on groundwater table fluctuations in unconfined aquifers. *Journal of Hydrology*, 528, 397-407. doi:10.1016/j.jhydrol.2015.06.045
- Kumar, M., Duffy, C. J., & Salvage, K. M. (2009). A Second-Order Accurate, Finite Volume-Based, Integrated Hydrologic Modeling (FIHM) Framework for Simulation of Surface and Subsurface Flow. *Vadose Zone Journal*, 8(4), 873-890. doi:10.2136/vzj2009.0014
- Maxwell, R. M., & Miller, N. L. (2005). Development of a Coupled Land Surface and Groundwater Model. *Journal of Hydrometeorology*, 6(3), 233-247. doi:10.1175/jhm422.1
- NCAR. (2018). The NCAR WRF-Hydro Modeling System Technical Description.
- Niu, G.-Y., Paniconi, C., Troch, P. A., Scott, R. L., Durcik, M., Zeng, X., . . . Goodrich, D. C. (2014). An integrated modelling framework of catchment-scale ecohydrological processes: 1. Model description and tests over an energy-limited watershed. *Ecohydrology*, 7(2), 427-439. doi:10.1002/eco.1362
- Niu, J., Shen, C., Chambers, J. Q., Melack, J. M., & Riley, W. J. (2017). Interannual Variation in Hydrologic Budgets in an Amazonian Watershed with a Coupled Subsurface-Land Surface Process Model. *Journal of Hydrometeorology*, 18(9), 2597-2617. doi:10.1175/jhm-d-17-0108.1

- Ponce, V. M., & Lugo, A. (2001). Modeling Looped Ratings in Muskingum-Cunge Routing. *Journal of Hydrologic Engineering*, 6(2), 119-124. doi:10.1061/(asce)1084-0699(2001)6:2(119)
- Tolikas, P. K., Sidiropoulos, E. G., & Tzimopoulos, C. D. (1984). A Simple Analytical Solution for the Boussinesq One-Dimensional Groundwater Flow Equation. *Water Resources Research*, 20(1), 24-28. doi:10.1029/wr020i001p00024
- USGS. (2012). NHDPlus Version 2: User Guide.
- Van Dam, J. C., & Feddes, R. A. (2000). Numerical simulation of infiltration, evaporation and shallow groundwater levels with the Richards equation. *Journal of Hydrology*, 233(1-4), 72-85. doi:10.1016/s0022-1694(00)00227-4
- Yeh, P. J. F., & Eltahir, E. A. B. (2005). Representation of Water Table Dynamics in a Land Surface Scheme. Part I: Model Development. *Journal of Climate*, 18(12), 1861-1880. doi:10.1175/jcli3330.1
- Zeng, Y. J., Xie, Z. H., Yu, Y., Liu, S., Wang, L. Y., Jia, B. H., . . . Chen, Y. N. (2016). Ecohydrological effects of stream-aquifer water interaction: a case study of the Heihe River basin, northwestern China. *Hydrology and Earth System Sciences*, 20(6), 2333-2352. doi:10.5194/hess-20-2333-2016